ISSN 0036-0295, Russian Metallurgy (Metally), Vol. 2023, No. 4, pp. 480–484. © Pleiades Publishing, Ltd., 2023.
Russian Text © The Author(s), 2022, published in Deformatsiya i Razrushenie Materialov, 2022, No. 10, pp. 28–33.

Deformation-Induced Transformation of the Lamellar Pearlite Structure in Rail Steel during Tension

K. V. Aksenova[a], V. E. Gromov[a, *], Yu. F. Ivanov[b], R. V. Kuznetsov[a], V. E. Kormyshev[a], and S. V. Vorob'ev[a]

[a] *Siberian State Industrial University, Novokuznetsk, 654007 Russia*
[b] *Institute of High-Current Electronics, Siberian Branch, Russian Academy of Sciences, Tomsk, 634055 Russia*
**e-mail: gromov@physics.sibsiu.ru*

Received April 28, 2022; revised May 17, 2022; accepted May 19, 2022

Abstract—The methods of modern physical materials science are used to study the defective substructure of lamellar pearlite and the properties of rail steel subjected to fracture under uniaxial tension. The ultimate tensile strength is found to be 1247–1335 MPa, and the relative strain to failure is 0.22–0.26. Three zones of fracture surface, i.e., fibrous, radial, and shear zones, are revealed. The deformation of rail steel is accompanied by the destruction of cementite plates in pearlite colonies and the repeated precipitation of tertiary cementite particles ≈8.3 nm in size in the volume of ferrite plates. The scalar dislocation density in ferrite increases from 3.2×10^{10} cm^{-2} in the initial state to 7.9×10^{10} cm^{-2} after fracture. Ferrite and cementite plates are fragmented. The average cementite fragment size is ≈9.3 nm.

Keywords: pearlitic rail steel, lamellar pearlite, plastic deformation, structure evolution, dislocation, cementite, fragmentation

DOI: 10.1134/S0036029523040031

INTRODUCTION

The considerable increase in the railroad traffic density in recent years and the growth of freight tonnage of railroad lines require a high operational durability of rails made of pearlitic steel. Rails in operation are subjected to significant deformation accompanied by the evolution of a lamellar pearlite structure [1–3]. The manufacturers of rails aim to create high-quality rails with high performance properties, which ensure accident-free operation for a passing tonnage of more than 2 billion gross tons. The wear resistance of rails can be improved by raising the purity of steel, increasing the carbon content [3], and hardening the rail head [3, 4].

The production of rails with low-temperature reliability and increased contact-fatigue endurance requires studying the dependence of their hardening on the initial structural state, establishing cause-and-effect relations between the phenomena that determine their strain behavior [5, 6].

Pearlitic steel rails in their initial state contain about 70% lamellar pearlite, the deformation of which is accompanied by a complex transformation of ferrite and cementite [5–8], usually observed by transmission electron microscopy. The main focus is on the deformation-induced fracture of cementite [8–10], which increases the carbon content in ferrite, contributing to additional hardening.

This work aims to analyze the deformation-induced transformation of the defect substructure of lamellar perlite in rail steel subjected to fracture under tension deformation conditions.

EXPERIMENTAL

Rail steel, the properties and element composition of which are regulated by GOST R 51685–2013 (Table 1), was the material of the study. Two-sided blades with a gage part 1.5 × 4.5 × 8.0 mm in size were cut from the head of differentially hardened DT350 grade rails manufactured by Evraz ZSMK from vacuum degassed E76KhF electric steel. Uniaxial tensile

Table 1. Chemical composition of rail steel, wt %

C	Mn	Si	Cr	P	S	Ni	Cu	Ti	Mo	V	Al
0.73	0.75	0.58	0.42	0.012	0.007	0.07	0.13	0.003	0.006	0.04	0.003

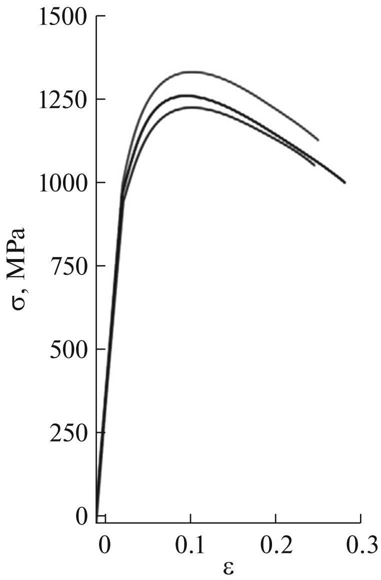

Fig. 1. Stress–strain curves of the rail steel subjected to uniaxial tension.

deformation was carried out using an Instron 3369 tester at a loading rate of 1.2 mm/min.

The structure of the fracture surface was examined by scanning electron microscopy using a SEM 515 Philips microscope. The defective substructure of the steel in the fracture zone was investigated by transmission electron microscopy using a JEOL JEM 2100 microscope [8–13]. Foils for transmission electron microscopy were prepared by argon ion thinning on an Ion Slicer EM-091001S of plates cut from fractured samples on an Isomet Low Speed Saw perpendicular to the fracture surface. The scalar and excess dislocation density measurement techniques were not different from those described in [5, 6].

RESULTS AND DISCUSSION

Figure 1 shows the stress–strain curves resulting from uniaxial tension of steel samples. The tests showed that the ultimate tensile strength is 1247–1335 MPa, and the strain to failure is 0.22–0.26.

Figure 2 shows typical images of the fracture surface of steel. As a rule, three zones are formed on the fracture surface during tensile deformation of specimens: a fibrous zone (in the central part of the specimen), a radial zone adjacent to it, and further, at the edge of the specimen, a shear zone [14]. The fibrous zone is elliptical in shape with a large axis parallel to the long sides of the specimen section (see Fig. 2a). The radial zone has a chevron, or "herringbone" shape (see Fig. 2b). Chevron patterns are often associated with unstable and relatively fast crack propagation. A chevron pattern appears due to the mismatch between the general direction of crack propagation and the shortest direction from the crack front to the free surface. Radial scars in this case propagate towards the free surface, forming chevron patterns [14]. The tops of the V-shaped chevrons are directed away from the fracture nucleus.

The following components are distinguished in the structure of the studied steel in terms of morphology [5, 6, 15]: lamellar pearlite, ferrite-carbide grains (degenerated pearlite) and structurally-free ferritic grains (ferritic grains with no carbide particles in their volume). The main structural components of the steel are lamellar pearlitic grains, the relative content of which is 0.7. The relative content of ferritic–carbide grains is 0.27. The rest (0.03) were structurally-free ferritic grains.

The structure of lamellar pearlite consists of alternating ferrite plates (solid solution of carbon in α-Fe, BCC crystal lattice) and cementite plates (iron carbide Fe_3C, orthorhombic crystal lattice) [16]. Fracture under uniaxial tension does not change the morphology of steel. There are grains with a lamellar structure

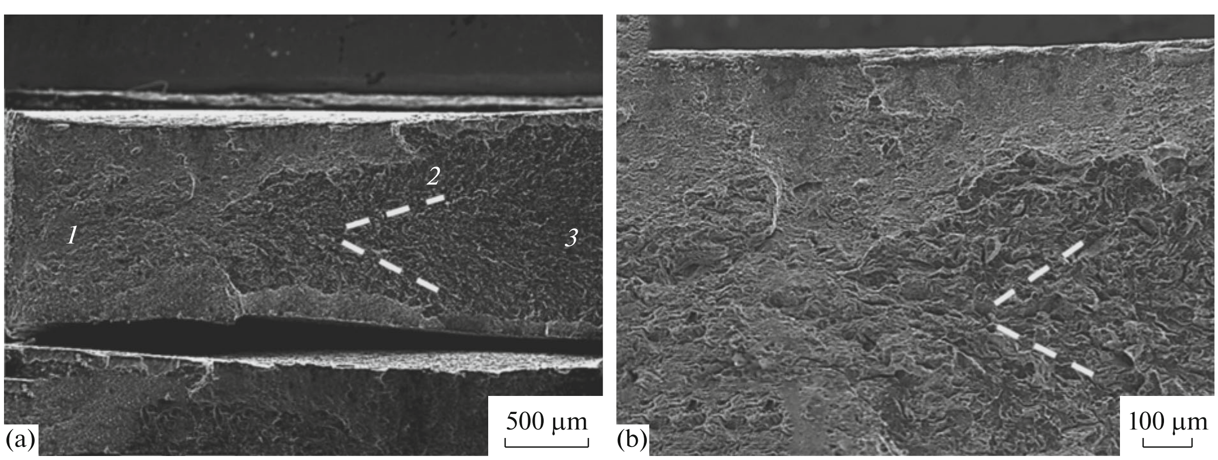

Fig. 2. Fracture surface of the rail steel: (*1*) shear region, (*2*) radial region (enlarged in (b)), and (*3*) fibrous region.

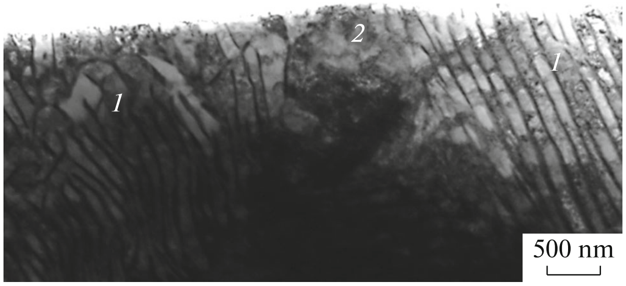

Fig. 3. Microstructure of the rail steel: (*1*) lamellar pearlite and (*2*) ferrite-carbide grains.

typical of pearlite in the fracture zone and away from it (Fig. 3). The transformation of the steel structure becomes apparent at the level of the defect subsystem and is accompanied by multiple pearlite transformations.

The ferritic plates of pearlitic colonies are found to be fragmented, i.e., split into regions separated by low-angle boundaries. The fragmentation of ferrite is best observed in dark-field analysis of the structure (Fig. 4).

The deformation involves the formation of a dislocation substructure in the volume of ferritic plates. Dislocations are chaotically distributed or form clusters. The scalar dislocation density is 7.9×10^{10} cm^{-2}. In the initial state it is 3.2×10^{10} cm^{-2}.

The deformation causes internal long-range stress fields in a specimen. Electron microscopy studies of thin foils reveal internal stress fields in the form of bending contours of extinction located mainly in ferritic plates. The sources of the stress fields in the steel are the interphase boundaries between the cementite and ferrite plates, as well as the grain boundaries. Note that the tensile strain of the steel is accompanied by the rotation of pearlite grains, which is most noticeable in the fracture zone of the specimens. This fact suggests the presence of a rotational mode of deformation in the fracture zone of the sample [17, 18]. Rotational modes of plastic deformation are associated with the formation of local lattice curvature. We can assume that this effect in the rail steel promotes the displacement of carbon atoms.

The deformation of the steel under study is also accompanied by the destruction of cementite plates. There are two possible mechanisms of their destruction discussed in the scientific literature, namely, cutting and dissolution [5, 6, 19]. Cementite plate dissolution is caused by higher bond energy of dislocations with carbon atoms (0.6–0.7 eV), and bond energy of carbon atoms in cementite lattice (≈0.4 eV) [20, 21]. The results of cementite fracture are interpreted thermodynamically in [22, 23]. An increase in free energy caused by geometric thinning of cementite plates and the formation of slip bands destabilizes the cementite and ensures its destruction [22]. A model based on the Gibbs–Thomson effect and the diffusion-controlled dissolution process is proposed in [23]. According to this model, carbon atoms are carried by moving dislocations into the volume of ferritic plates to form nanoscale particles of iron carbide. The average size of particles located in the ferritic plates is 8.3 nm. The particles of this size can be observed using the technique of dark-field analysis.

The dissolution of the cementite results in some material around the plates, which differs in contrast from the main grain volume. We can assume that the contrast changes due to a change in the chemical composition of the material surrounding the cementite

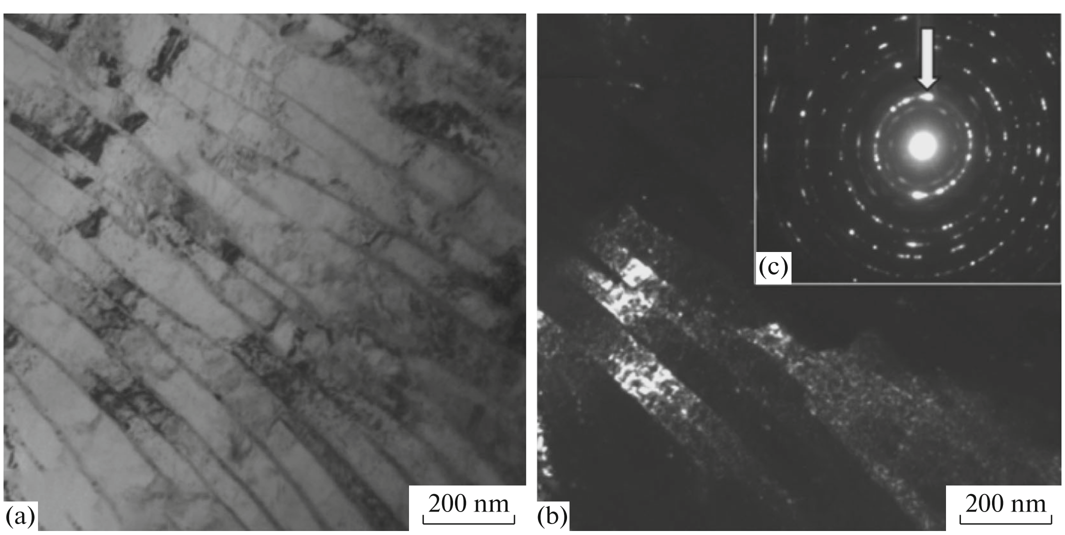

Fig. 4. Fragmented structure of ferrite: (a) bright-field image and (b) dark-field image taken in the [110]α-Fe reflection (shown by arrow in (c)).

plate, particularly, the higher concentration of carbon. Carbon atoms drawn out of cementite by dislocations can form Cottrell atmospheres, changing the contrast.

In addition to the dissolution of cementite plates, the plastic deformation of steel goes hand in hand with their fragmentation. The cementite plates in the fracture zone of the specimens are found to break up into nanoscale fragments (≈9.3 nm), retaining their original morphology.

The results of this work are quite comparable with those of the studies on the structure of rail steel after compression deformation up to 50% [24]. The strain hardening has a multistage character and occurs with the fragmentation of pearlitic grains, which increases with the strain degree and reaches ≈0.4 volume of the studied foil at $\varepsilon = 50\%$. The cementite plates fracture according to the mechanisms of their dissolution and cutting by mobile dislocations, with the formation of tertiary cementite particles 2–4 nm in size.

CONCLUSIONS

(1) The ultimate tensile strength of pearlitic rail steel is 1247–1335 MPa, and the strain to failure is 0.22–0.26.

(2) The deformation of steel is accompanied by the fragmentation of ferritic plates by low-angle boundaries and a significant increase in the scalar dislocation density to 7.9×10^{10} cm^{-2} (scalar dislocation density of the initial steel is 3.2×10^{10} cm^{-2}).

(3) We revealed the fracture of cementite plates by cutting and dissolution mechanisms followed by carbon removal by moving dislocations into ferrite plates to form nanosized (8.3 nm) round-shaped tertiary cementite particles.

(4) The dissolution of cementite plates is accompanied by their fragmentation, i.e., separation into coherent scattering regions with an average size of 9.3 nm.

ACKNOWLEDGMENTS

We thank E.V. Polevoi for supplying the rail steel samples and N.A. Popova for helfull discussion.

FUNDING

This work was supported by the Russian Foundation for Basic Research (project no. 19-32-60001) and the Russian Presidential Scholarship for Young Scientists and PhD Students Engaging in Promising Scientific Research and Development Focused on Priority Areas of Modernizing the Russian Economy (project SP-4517.2021.1).

CONFLICT OF INTEREST

The authors declare that they have no conflicts of interest.

REFERENCES

1. K. Labisz and J. Konieczny, "Natural ageing effects on microstructure and properties of rail fastening elements SKL12," Sci. J. Silesian Univ. Technol. Ser. Transp. **106** 79–90 (2020).
2. J. Konieczny and K. Labisz, "Structure and properties of the S49 rail after a long term outdoor exposure," Adv. Sci. Technol. Res. J. **16** (2), 280–290 (2022).
3. M. Masoumi, E. A. Ariza, A. Tschiptschin, and H. Goldenstein, "Improvement of wear resistance in a pearlitic rail steel via quenching and partitioning processing," Sci. Rep. **9** (1), 7454 (2019).
4. T. Zygmunt, M. Pietrzyk, Ł. Rauch, and D. Bachniak, "Optimization of the heat treatment process to obtain the required distribution of mechanical properties in the rail head of pearlitic rails," J. Met. Mater. **71** (1), 3–9 (2019).
5. A. A. Yuriev, Yu. F. Ivanov, V. E. Gromov, Yu. A. Rubannikova, M. D. Starostenkov, and P. Y. Tabakov, *Structure and Properties of Lengthy Rails after Extreme Long-Term Operation* (Materials Research Forum, Millersville, 2021).
6. V. E. Gromov, O. A. Peregudov, Yu. F. Ivanov, S. V. Konovalov, and A. A. Yur'ev, *Evolution of Structural and Phase States of Rail Metal during Long-Term Operation* (Sib. Otd. Ross. Acad. Nauk, Novosibirsk, 2017).
7. Y. Ivanisenko, R. Kulagin, V. Fedorov, A. Mazilkin, T. Scherer, B. Baretzky, and H. Hahn, "High pressure torsion extrusion as a new severe plastic deformation process," Mater. Sci. Eng., A **664**, 247–256 (2016).
8. F. Fang, Y. Zhao, P. Liu, L. Zhou, X. Hub, X. Zhou, and Z. Xie, "Deformation of cementite in cold drawn pearlitic steel wire," Mater. Sci. Eng., A. **608**, 11–15 (2014).
9. Jiang-li Ning, E. Courtois-Manara, L. Kurmanaeva, A. V. Ganeev, R. Z. Valiev, C. Kübel, and Yu. Ivanisenko, "Tensile properties and work hardening behaviors of ultrafine grained carbon steel and pure iron processed by warm high pressure torsion," Mater. Sci. Eng., A. **581**, 8–15 (2013).
10. P.-Y. Tung, X. Zhou, D. Mayweg, L. Morsdorf, and M. Herbig, "Under-stoichiometric cementite in decomposing binary Fe–C pearlite exposed to rolling contact fatigue," Acta Mater. **216**, 117144 (2021).
11. F. R. Egerton, *Physical Principles of Electron Microscopy* (Springer, Basel, 2016).
12. C. S. S. R. Kumar, *Transmission Electron Microscopy. Characterization of Nanomaterials* (Springer, New York, 2014).
13. C. B. Carter and D. B. Williams, *Transmission Electron Microscopy* (Springer, Berlin, 2016).
14. *Fractography and Atlas of Fractographs. Handbook*, Ed. by J. A. Fellows, (Metals Park, OH, 1974).
15. R. V. Kuznetsov, V. E. Gromov, Yu. F. Ivanov, V. E. Kormyshev, Yu. A. Shlyarova, E. V. Polevoi, and A. A. Yur'ev, "Evolution of structural-phase states and properties of differentially hardened rails during long-term operation," Probl. Chernoi Metall. Materialoved., No. 3, 37–46 (2021).

16. V. M. Schastlivtsev, A. A. Mirzaev, I. L. Yakovleva, K. Yu. Okishev, T. I. Tabatchikova, and Yu. V. Khlebnikova, *Perlite in Carbon Steels* (Ural. Otd. Ross. Akad. Nauk, Ekaterinburg, 2006).
17. V. E. Panin, V. E. Egorushkin, A. V. Panin, and A. G. Chernyavskii, "Plastic distortion as a fundamental mechanism in nonlinear mesomechanics of plastic deformation and fracture," Phys. Mesomech. **19** (3), 255–268 (2016).
18. K. V. Grigorovich, V. E. Gromov, R. V. Kuznetsov, Yu. F. Ivanov, and Yu. A. Shlyarova, "Fine structure formation of pearlitic steel under ultra-long plastic deformation," Dokl. Akad. Nauk **503**, 8–12 (2022).
19. Y. J. Li, P. Choi, C. Borchers, S. Westerkamp, S. Goto, D. Raabe, and R. Kirchheim, "Atomic-scale mechanisms of deformation-induced cementite decomposition in pearlite," Acta Mater. **59**, 3965–3977 (2011).
20. V. G. Gavriljuk, "Effect of interlamellar spacing on cementite dissolution during wire drawing of pearlitic steel wires," Scr. Mater. **45**, 1469–1472 (2001).
21. V. G. Gavriljuk, "Decomposition of cementite in pearlite steel due to plastic deformation," Mater. Sci. Eng., A **345**, 81–89 (2003).
22. J. Languillaume, G. Kapelski, and B. Baudelet, "Cementite dissolution in heavily cold drawn pearlitic steel wires," Acta Mater. **45** (3), 1201–1212 (1997).
23. X. Sauvage, J. Copreaux, F. Danoix, and D. Blavette, "Atomicscale observation and modelling of cementite dissolution in heavily deformed pearlitic steels," Philos. Mag. A **80**, 781–796 (2000).
24. Yu. F. Ivanov, V. E. Gromov, K. V. Aksenova, R. V. Kuznetsov, V. E. Kormyshev, and E. S. Vashchuk, "Evolution of the structure of rail steel during compression," Russ. Metall. (Metally) **2022**, 1192–1197 (2022).

Translated by T. Gapontseva